PHYSICAL REVIEW E **73**, 055201(R) (2006)

Frequency versus relaxation oscillations in a semiconductor laser with coherent filtered optical feedback

H. Erzgräber,[1] B. Krauskopf,[2,1] D. Lenstra,[1,3] A. P. A. Fischer,[4] and G. Vemuri[5]
[1]*Afdeling Natuurkunde en Sterrenkunde, Vrije Universiteit Amsterdam, 1081 HV Amsterdam, The Netherlands*
[2]*Department of Engineering Mathematics, University of Bristol, Bristol BS8 1TR, United Kingdom*
[3]*Research Institute COBRA, Technical University Eindhoven, The Netherlands*
[4]*Laboratoire de Physique des Lasers, Université Paris XIII, UMR CNRS 7538, France*
[5]*Indiana University–Purdue University Indianapolis, Indiana 46202-3273, USA*
(Received 16 November 2005; published 24 May 2006)

We investigate the dynamics of a semiconductor laser subject to coherent delayed filtered optical feedback. A systematic bifurcation analysis reveals that this system supports two fundamentally different types of oscillations, namely relaxation oscillations and external roundtrip oscillations. Both occur stably in large domains under variation of the feedback conditions, where the feedback phase is identified as a key quantity for controlling this dynamical complexity. We identify two separate parameter regions of stable roundtrip oscillations, which occur throughout in the form of pure frequency oscillations.

DOI: 10.1103/PhysRevE.73.055201 PACS number(s): 42.65.Sf, 05.45.Xt, 02.30.Ks, 42.55.Px

We consider a semiconductor laser with filtered optical feedback (FOF), where the output light re-enters the laser after passing through a filter of a given central frequency and width. FOF has received attention recently, because of the additional control over the behavior of the laser by choosing the filter width and the detuning between the laser and the filter [1–3]. Recently, in Ref. [2], the observation of so-called frequency oscillations (FOs) was reported—oscillations for which the laser intensity is almost constant, only the laser frequency oscillates. This experimental observation triggered a vivid discussion. While FOs were found by numerical integration for certain values of the parameters of an appropriate rate equation model, their characterization and stability properties remained unclear. Here, we identify the feedback phase and the feedback rate as important parameters, and give a comprehensive and complete picture of the mechanism leading to stable FOs. We show that these FOs belong to the wider class of external roundtrip oscillations.

Filtered optical feedback is an example of coherent feedback, where both the amplitude and phase of the feedback are important. The feedback signal accumulates a feedback phase $C_p=\Omega_0\tau$, where Ω_0 is the laser frequency and τ is the delay time. C_p controls the position of the solitary laser frequency Ω_0 with respect to the optical frequency comb of the external delay system, which is quite similar to the carrier off-set frequency in laser-based precision spectroscopy and optical frequency comb techniques [4]. This is in contrast to optical systems with incoherent feedback [3,5–7] since these systems lack an underlying external frequency comb. For the case of conventional optical feedback, it turns out that for sufficiently long delay times, the external cavity mode spacing $\nu_{\mathrm{EC}}\sim 1/\tau$ becomes very small and the number of modes increases so much that C_p has no influence anymore. However, for short delay times (on the order of or less than the characteristic relaxation oscillation period) C_p becomes a key parameter [8–10]. We demonstrate here that C_p is important for the dynamics of the FOF laser even for relatively long delay times (larger than the relaxation oscillation period). This is because the number of modes is reduced drastically by the narrow filter linewidth. In particular, C_p distinguishes between the large number of coexisting stable solutions.

The FOF laser has been studied by numerical integration of the governing rate equations (introduced below), which showed the existence of periodic, quasiperiodic, and chaotic output, as well as good agreement between the rate equations and experiments [11,12]. How the continuous-wave (cw) solutions—known as the external filtered modes (EFMs)—depend on the parameters is analyzed in Ref. [13].

We report here on qualitatively different types of oscillations of the FOF laser, which bifurcate when the EFMs lose their stability. In particular, we consider stable external roundtrip oscillations, and show that they have almost constant intensity, which identifies them as the FOs that were reported in Ref. [2]. The existence of FOs is remarkable because the phase-amplitude coupling in semiconductor lasers should lead to an intimate connection between intensity and phase oscillations. While external roundtrip oscillations, in general, may have intensity variations as well, we show that stable FOs form a continuous subset that occurs stably in large regions of the parameter space. We also study the much better known relaxation oscillations (ROs), which are a periodic exchange of energy between the electric field and the inversion inside the laser at a frequency that is influenced only little by the delay; see, e.g., Refs. [14,15].

In the coherent FOF setup, shown in Fig. 1, a part of the light emitted by the laser is spectrally filtered by a Fabry-Pérot interferometer and then reinjected into the laser after a

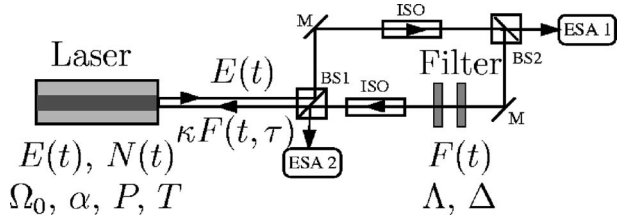

FIG. 1. Experimental setup with the laser and the feedback loop with a Fabry-Pérot, beamsplitter (BS), optical isolator (ISO), mirrors (M), and electrical spectrum analyzer (ESA) for measuring the laser (ESA 1) and feedback light (ESA 2).

fixed delay time. At BS1, 50% of the light emitted by the laser enters the feedback loop, where optical isolators allow clockwise propagation only. The Fabry-Pérot with a finesse of ~5 is made of two parallel mirrors resulting in a transmission line shape that is approximated by a single Lorentzian. A pigtailed photodiode, an amplifier with a bandwidth of 500 MHz, and an ESA are used to measure the dynamics of both the intensity emitted by the laser and the intensity fed back into it. Great care has been taken to prevent unwanted feedback from the detection branches.

The FOF laser can be modeled by the rate equations

$$\dot{E} = (1 + i\alpha)N(t)E(t) + \kappa F(t,\tau), \tag{1}$$

$$T\dot{N} = P - N(t) - (1 + 2N(t))|E(t)|^2, \tag{2}$$

$$\dot{F} = \Lambda E(t-\tau)e^{-iC_p} + (i\Delta - \Lambda)F(t), \tag{3}$$

where time is measured in units of the photon lifetime (of 10 ps), E and F are the complex envelopes of the optical field of the laser and filtered feedback field, respectively, and N is the inversion of the laser; see also Ref. [13]. The parameters are the self-phase modulation α, the feedback rate κ, the carrier life time T, the half-width at half-maximum (HWHM) of the filter Λ, the feedback phase C_p, the delay time τ, and the detuning Δ between the laser and the filter. These rescaled parameter values are chosen to represent the experimental conditions, namely $\alpha=5.0$, $\tau=500$, $\Lambda=0.007$, $\Delta=-0.007$, $T=100$, and $P=3.5$.

We present an extensive bifurcation analysis of system (1)–(3) and determine the stability of EFMs, ROs, and FOs as a function of the feedback rate κ and the feedback phase C_p. For this purpose, we use the continuation software DDE-BIFTOOL [16]. Continuation has the advantage over numerical simulation that it is not affected by the problems of finding suitable initial conditions and dealing with transient behavior [17].

Figure 2 depicts time series of ROs (a), FOs (b), and quasi-periodic frequency oscillations (c). Shown are the intensities $I_{L,F}$ and the frequencies $\dot{\Phi}_{L,F}$ of the laser field and the feedback field, respectively, where $E(t)=\sqrt{I_L(t)}e^{i\Phi_L(t)}$ and $F(t)=\sqrt{I_F(t)}e^{i\Phi_F(t)}$. Figure 2(a) shows a typical example of ROs with a frequency of 4.2 GHz. (In an optical spectrum, such ROs can be seen as side peaks.) Since the HWHM of the filter is narrow compared to the relaxation oscillation frequency, the intensity I_F transmitted through the filter (and then fed back into the laser) is almost constant. Effectively, the laser experiences constant weak optical injection that undamps the ROs.

That the dynamics of the filter has to be taken into account for an intermediate filter width as discussed here is evidenced by the presence of FOs, of which Fig. 2(b) shows an example. In contrast to the ROs, the intensity of the laser is almost constant, but its frequency $\dot{\Phi}_L$ oscillates with a period related to the roundtrip time in the feedback loop. (The period is actually longer because the filter adds a substantial frequency shift of $\sim 1/\Lambda$.) The roundtrip time $\tau = 5$ ns corresponds to a frequency of 200 MHz, which is well

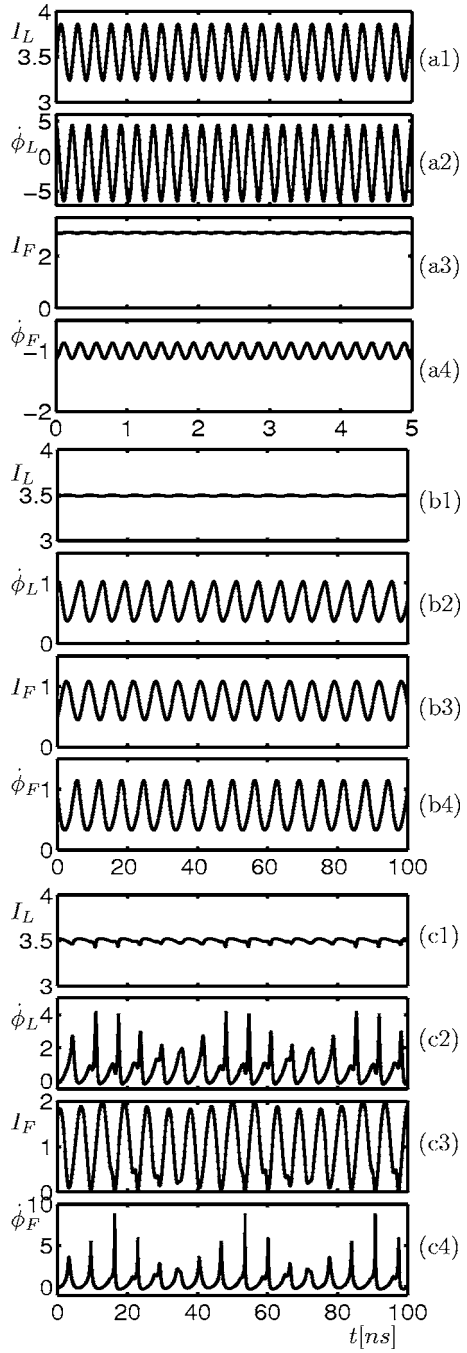

FIG. 2. Time series of I_L, I_F $\dot{\Phi}_L$, and $\dot{\Phi}_F$ of ROs (a), FOs (b), and quasi-periodic FOs (c). From (a) to (c) (κ, C_p) takes the values $(0.02, -8/3\pi)$, $(0.07, -6\pi)$, and $(0.014, -6\pi)$.

within the filter width. Thus, both I_F and $\dot{\Phi}_F$, and therefore the instantaneous feedback rate and phase, are oscillating. Note that the laser frequency $\dot{\Phi}_L$ and the feedback intensity I_F are approximately in antiphase for this FO. In Ref. [2], the FOs are interpreted as an interplay between the filter and the laser that compensates for the effects of the amplitude-phase coupling, leading to an effectively zero α-parameter. Also, in Ref. [1] it is argued that FOF, in this case from a double mirror, effectively reduces the value of α. Figure 2(b) allows us to characterize this interplay in more detail. Because of

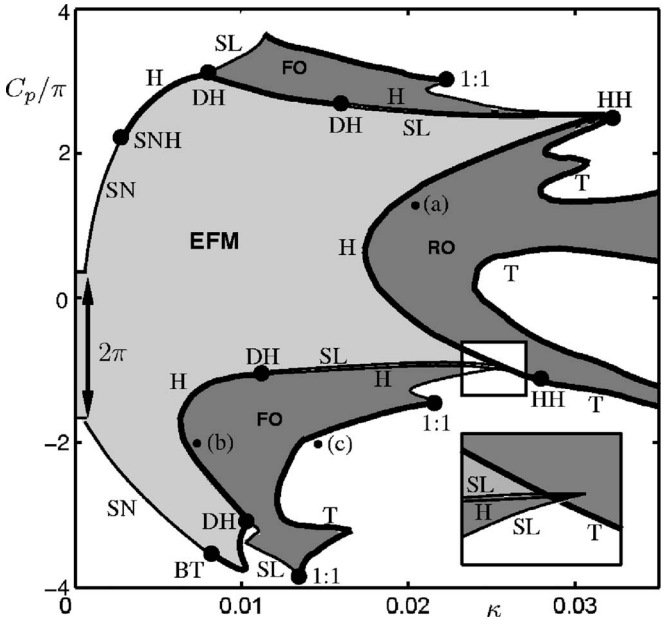

FIG. 3. Regions of different dynamics in the (κ, C_p)-plane with stable EFMs (light gray) and stable FOs or ROs (dark gray). Bifurcation curves are saddle-node (SN), saddle-node of limit cycle (SL), Hopf (H), and torus (T) bifurcations. Codimension-two points are Bogdanov-Takens (BT), saddle-node Hopf (SNH), degenerate Hopf (DH), 1:1 resonance (1:1), and double Hopf (HH) points. The points (a)–(c) indicate the parameter values of the time series of Fig. 2. The inset shows an enlarged view at the tip of the lower FO region.

the filter the intensity of the feedback light changes according to the changes in the frequency of the laser. This results in a virtually constant intensity of the laser.

Finally, Fig. 2(c) shows that FOs can undergo further bifurcations, e.g., a torus bifurcation. This dynamical regime differs from the quasiperiodic dynamics associated with ROs, in that there is again only very small intensity dynamics. Notice that the FOs exhibit a slow modulation with a period about six times larger than the basic oscillation. This ratio may crucially depend on other parameters.

Figure 3 shows the stability regions of EFMs, and the bifurcating ROs and FOs in the (κ, C_p) plane. Specifically, starting from the solitary laser state, a single EFM is followed in κ and C_p. The resulting stability regions extend over several 2π- cycles of C_p. Due to the periodicity of C_p, all 2π-shifted copies of these stability regions coexist, which leads to a large amount of multistability. It is possible that up to four stable EFMs coexist with ROs and the two kinds of FOs.

There is one large region of stable EFMs (light gray) and three large regions of stable oscillations (dark gray), namely one region of stable ROs and two regions of stable FOs. Notice that FOs appear for much lower values of κ. The FOs shown in Fig. 2(b) are from the lower region and feature an approximate antiphase relationship between $\dot{\Phi}_L(t)$ and $I_F(t)$, because they involve the right flank of the filter profile. In the upper region of FOs, on the other hand, they involve the left flank of the filter profile, and $\dot{\Phi}_L(t)$ and $I_F(t)$ are approximately in phase. For the parameters chosen here, the intensity of the laser varies less than 1.5% from its average value throughout the entire FO stability regions.

The boundaries in Fig. 3 are bifurcation curves, where the dynamics changes qualitatively. Typically, EFMs are created in pairs in saddle-node bifurcations (SN) and lose their stability in Hopf bifurcations (H). In Fig. 3, we only plot bifurcation curves that correspond to bifurcations of stable EFMs. The boundary type changes at codimension-two points, namely at Bogdanov-Takens (BT) and saddle-node Hopf points (SNH) [18]. Depending on κ and C_p, either ROs or FOs are born in the loss of stability of EFMs. In turn, ROs and FOs can bifurcate in saddle-node bifurcations of limit cycles (SL) or lose their stability in a torus bifurcation (T). Again only bifurcations of stable ROs and FOs are plotted, and the stability boundary may change at codimension-two points, namely at degenerate Hopf points (DH), at 1:1 resonances (1:1), and double Hopf points (HH) [18]. Parts of the Hopf curves that give rise to FOs are subcritical, but immediately followed by SL bifurcations where the FOs become stable; both types of curves are practically on top of each other in Fig. 3. Notice also the tiny overlap (see inset) between the stability region of FOs and that of EFMs and ROs. A torus bifurcation T leads to quasiperiodic dynamics as is shown for an FO in Fig. 2(c). Beyond T, the unstable FOs can be followed to detect further bifurcations, and we found that they may undergo period doubling.

Figure 4 shows experimental RIN-spectra of stable FOs, where the length of the feedback loop was measured to be $L=1.55\pm0.01$ m, corresponding to a roundtrip frequency of $f_{\text{ext}}=193\pm1$ MHz. The filter HWHM was 900 MHz. Figure 4(a) shows the RIN of the intensity emitted by the laser

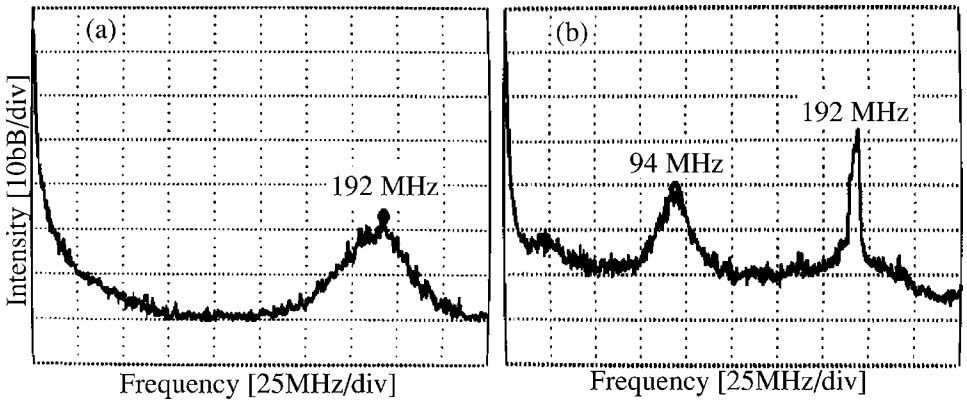

FIG. 4. Experimental RIN spectra of FOs: Intensity (a) and frequency measured as the feedback intensity (b) of the laser.

(ESA 1), and Fig. 4(b) shows the RIN of the intensity fed back into the laser (ESA 2). Both spectra have a peak T1 at 192 MHz, which is at f_{ext} within the experimental accuracy. The linewidth of the peak in Fig. 4(a) is very broad (about 20 MHz). Therefore, we interpret it as noise-enhanced dynamics of an unstable resonance condition in the feedback loop. The peak in Fig. 4(b), on the other hand, is very narrow and about 20 dB higher. These are clear FOs, converted into intensity by the operation of the filter and detected by the photodiode. Together these RIN spectra constitute the characteristics of the theoretical FO dynamics in Fig. 3(b). The RIN in Fig. 4(b) also shows a smaller broad peak T2 at 94 MHz. Since T1 and T2 are in a ratio of 1:2 within the experimental accuracy, this might suggest a noise-induced precursor of a (possibly unstable) period-doubled solution.

In conclusion, we showed that a semiconductor laser with filtered optical feedback supports fundamentally different oscillations, namely two kinds of pure frequency oscillations and characteristic relaxation oscillations. Both occur stably in large domains under variation of the feedback conditions. The feedback phase was recognized as the main distinguishing parameter. Our analysis characterizes the FOs in terms of the interplay between the laser field and the feedback field. We found two separate regions of FOs that differ in that the laser-field frequency and the filtered field intensity are in phase and antiphase, respectively. The detailed analysis of FOs and their bifurcations is an interesting topic of ongoing investigations; an immediate question is why FOs are supported for much lower values of the feedback strength than ROs. Another interesting challenge is the study of more complicated dynamics, including quasi-periodicity and chaos, that are possible when FOs become unstable.

ACKNOWLEDGMENTS

G.V. was supported by the NSF, B.K. by EPSRC Grant No. GR/A11649/01, and A.F. by Access to the Research Infrastructure Grant No. HPRI-CT-1999-00064, project 1035, of LaserCentreVU.

[1] F. Rogister, P. Mégret, O. Deparis, M. Blondel, and T. Erneux, Opt. Lett. **24**, 1218 (1999).
[2] A. P. A. Fischer, M. Yousefi, D. Lenstra, M. W. Carter, and G. Vemuri, Phys. Rev. Lett. **92**, 023901 (2004).
[3] H. Yasaka and H. Kawagushi, Appl. Phys. Lett. **53**, 1360 (1988).
[4] Th. Udem, R. Holzwarth, and T. W. Hänsch, Nature (London) **416**, 233 (2002).
[5] T. Heil, A. Uchida, P. Davis, and T. Aida, Phys. Rev. A **68**, 033811 (2003).
[6] B. Farias, T. Passerat deSilans, M. Chevrollier, and M. Oriá, Phys. Rev. Lett. **94**, 173902 (2005).
[7] L. Larger, P.-A. Lacourt, S. Poinsot, and M. Hanna, Phys. Rev. Lett. **95**, 043903 (2005).
[8] T. Heil, I. Fischer, W. Elsäßer, and A. Gavrielides, Phys. Rev. Lett. **87**, 243901 (2001).
[9] O. Ushakov, S. Bauer, O. Brox, H.-J. Wünsche, and F. Henneberger, Phys. Rev. Lett. **92**, 043902 (2004).
[10] A. Tabaka, K. Panajotov, I. Veretennicoff, and M. Sciamanna, Phys. Rev. E **70**, 036211 (2004).
[11] A. Fischer, O. Andersen, M. Yousefi, S. Stolte, and D. Lenstra, IEEE J. Quantum Electron. **36**, 375 (2000).
[12] M. Yousefi, D. Lenstra, and G. Vemuri, Phys. Rev. E **67**, 046213 (2003).
[13] K. Green and B. Krauskopf, Opt. Commun. **258**, 243 (2006).
[14] A. Tager and K. Petermann, IEEE J. Quantum Electron. **30**, 1553 (1994).
[15] B. Haegeman, K. Engelborghs, D. Roose, D. Pieroux, and T. Erneux, Phys. Rev. E **66**, 046216 (2002).
[16] K. Engelborghs, T. Luzyanina, and G. Samaey, DDE-BIFTOOL v. 2.00 user manual. Technical report TW-330 (Department of Computer Science, K.U. Leuven, Leuven, Belgium, 2001).
[17] B. Krauskopf, in *Unlocking Dynamical Diversity: Optical Feedback Effects on Semiconductor Lasers*, edited by D. Kane and K. Shore (Wiley, New York, 2005), pp. 147–183.
[18] Y. Kuznetsov, *Elements of Applied Bifurcation Theory* (Springer, New York, 1995).